Nanomechanics, Tribology and Nanostructures

Mater. Res. Soc. Symp. Proc. Vol. 1049 © 2008 Materials Research Society 1049-AA02-04

Comprehensive Mechanical and Tribological Characterization of Ultra-Thin-Films

Norm Gitis, Michael Vinogradov, Ilja Hermann, and Suresh Kuiry
Center for Tribology, Inc., 1715 Dell Ave, Campbell, CA, 95008

ABSTRACT

Mechanical and tribological properties such as hardness, Young's modulus, friction, and scratch adhesion strength of various coatings and ultra-thin films are reported. These results, obtained using a Universal Nano+Micro Tester UNMT-1, indicate that a substrate effect for ultra-thin films is substantial when using conventional static nanoindentation technique, while negligible with an advanced dynamic nano-indentation. Comparative results of hardness and Young's modulus obtained from various techniques are presented. A means to evaluate friction and adhesion strength of thin films is highlighted, using DLC specimens as an example.

INTRODUCTION

Evaluation of mechanical and tribological properties of bulk and coating materials is of great importance for design and development of engineering components with enhanced structural and wear performance [1-3]. Traditional indentation tests of bulk materials include macro-hardness measurements at high loads of the order of kN. Micro-hardness measurements of coatings and bulk materials are usually performed under loads of the order of N. As the industrial technology advanced, the characterization technique for mechanical properties of thin films and coating shifted its range to mN and even μN.

In recent years, nano-indentation has become a popular technique for evaluation of hardness and Young's modulus of films and coatings. The nature of stress distribution in the front of a nano-indenter tip makes the indentation vulnerable to a substrate effect. Usually, the indentation depth should be restricted to 5 - 10% of the film thickness to limit the stress field within the thickness of the film and thus, to avoid the substrate influencing the results of such measurements. Such measurements at ultra-shallow depths would require an extremely high accuracy of both depth monitoring and tip calibration. Although AFM-based nano-indentation shows some potential to circumvent such problem, the use of compliant tips limits its applications to soft materials. A novel Nano-analyzer enables quantitative characterization of ultra-thin films, including hard and super-hard films, at shallow depths with a negligible substrate effect.

Primary objective of the present investigation is to compare different techniques to perform mechanical and tribological tests on micro and nano-level using a single tester.

EXPERIMENTAL

The micro-indentation, micro-scratch, nano-indentation, nano-scratch, and nano-imaging techniques were employed for evaluation of mechanical and tribological properties of numerous bulk, coating and film specimens using the same Universal Nano+Micro Tester model UNMT-1, designed and manufactured by CETR, Inc. The photograph of its nano-head is presented in Figure 1.

UNMT-1 has several easily interchangeable modules for precision tests of hardness, Young's modulus, friction, and adhesion of bulk, coating and film materials, including:

- traditional micro-indentation up to a load of 1.2 kN, with Rockwell, Vickers, and Knoop indenters according to ASTM E18-05, ASTM E92-82, and ASTM E384-99 standards,

respectively. It can perform post-test measurements of diagonals of indentation with an optical microscope as required by Vickers and Knoop hardness test procedures, and of indentation depth with a capacitance sensor for Rockwell hardness test,

- instrumented micro-hardness tests per the ISO 14577-1/02 up to a load of 1.2 kN with the same Rockwell, Vickers, or Knoop indenters, but *in-situ* monitoring of load and depth and automatic calculations of both instrumented hardness and Young's modulus,

- instrumented static nano-indentation tests per the ISO 14577-1/02 (loads from 0.1 μN to 0.5 N) with Berkovich, conical and cube-corner indenters, *in-situ* monitoring of load and displacement and automatic calculations of both instrumented hardness and Young's modulus,

- instrumented dynamic Young's modulus tests with spherical, Berkovich, and other indenters, *in-situ* monitoring of tip frequency changes during surface scanning, and both calculations and maps of Young's modulus,

- micro-scratch-hardness tests per the ASTM G171-03 (loads from centi-N to hecto-N, sliding distances from a few microns to many millimeters) with numerous indenters (spherical, conical, micro-blades, etc.), under a constant load or any other loading profile with capability of simultaneous monitoring of friction, acoustic emission, electrical resistance, etc.

- nano-scratch-hardness tests per the ASTM G171-03 (loads from 0.1 micro-N to hecto-N, sliding distances from 1 to 100 microns) with numerous indenters (Berkovich, spherical, etc.) and AFM-like imaging of scratches with the same tip.

The UNMT-1 allows for multi-scale measurements of the same sample without its removal, just with an easy exchange of the mentioned indentation and scratch modules.

RESULTS AND DISCUSSION

The evaluation results of mechanical and tribological properties of numerous specimens in ambient conditions are summarized in Table 1. Whereas the "+"shows that the technique was sufficient to measure the property of the sample, the "–"indicates that the technique failed to evaluate the film properties without the substrate effect.

Table 1: Summary of hardness tests performed using UNMT-1

Specimens	Micro-indentation		Instrumented		
	Traditional	Instrumented	Micro-scratch	Nano-indentation	Nano-scratch
Bulk Materials	+	+	+	+	+
20μm metallic film	–	+	+	+	+
2μm metallic film	–	–	+	+	+
4 nm DLC film	–	–	–	–	+

Micro-indentation

Instrumented indentation tests were performed on bulk metal specimens with a Rockwell diamond indenter with tip radius of 200 micron. The maximum loads for aluminum, brass, and steel specimens were about 30, 70 and 150 N, respectively. Figure 2 shows the representative load-displacement plots, the unloading portions of which were analyzed using the Oliver-Pharr methodology [4]. Table 2 presents the mean hardness and Young's modulus values, obtained

from 20 tests on each specimen. It also shows the average value of 20 hardness data obtained from traditional Vickers hardness test on the same samples. The average results of the instrumented and traditional techniques were practically the same (the 10-time difference is due to the Vickers scale), while the deviation in hardness values were found to be less in instrumented indentation compared to the traditional Vickers hardness test.

Fig. 1. Nano-indentation module for UNMT-1

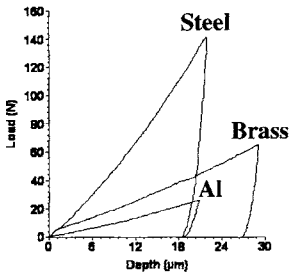

Fig. 2. Load-displacement plots for metals

Micro-Scratch

The instrumented micro-scratch tests included sliding-scratching over 5 mm length at a speed of 0.2 mm/s under a constant load, using a Rockwell diamond indenter, on test specimens and a reference material. The scratching loads for the specimen (F_S) and the reference (F_R) should be such that the scratch widths should be similar. The scratch hardness (HS) is:

$$HS = H_R \cdot \frac{F_S}{F_R}\left(\frac{W_R}{W_S}\right)^2 \qquad \text{.....(1)}$$

H_R is the hardness of the reference material, W_R and W_S are the scratch widths on the reference and specimen, respectively. Table 3 shows the scratch width and hardness on the fused silica, bare and coated metal; the coating exhibited hardness three times higher than the substrate.

Table 2: Hardness and modulus for aluminum, brass and steel specimens

Specimen	Hardness, MPa	Young's modulus, GPa	Vickers hardness
Aluminum	968±23	74±2	97±11
Brass	2004±19	127±2	201±9
Steel	5202±47	195±8	519±20

Table 3: Scratch hardness on fused silica, bare and coated specimens

Sample	Load, N	Scratch width, μm						Hardness, GPa
		1	2	3	4	5	Mean	
Fused Silica	0.2	9.96	9.78	9.68	10.23	10.03	**9.94**	9.5
Coating	0.1	7.74	7.79	7.83	8.23	7.98	**7.91**	7.5
Substrate	0.1	13.75	13.64	13.65	13.86	14.05	**13.79**	2.4

Static and Dynamic Nano-indentation

Instrumented nano-indentation was performed in both static and dynamic modes, using the same Berkovich indenter. Figures 3 and 4 show ten load-displacement curves obtained from static nano-indentation tests on a fused silica and 2-μm polymer coating on silicon. Figure 5 presents ten frequency-approach curves obtained from dynamic nano-indentation on reference polycarbonate specimen and on the 2-μm polymer film on silicon. One can see excellent data repeatability of both sets of data.

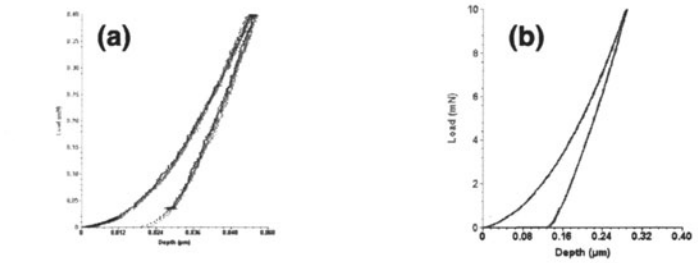

Fig. 3. Load-displacement curves on fused silica up to (a) 0.4 mN and (b) 10 mN.

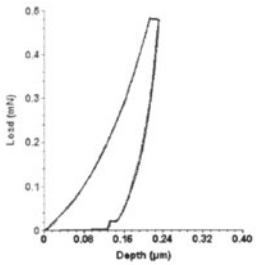

Fig. 4. Load-displacement curves into 2 μm polymer on Si.

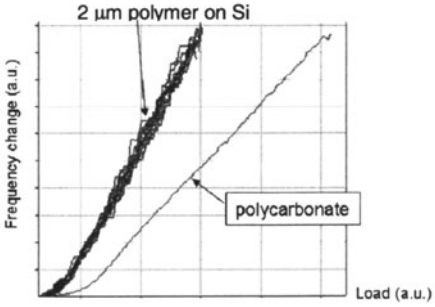

Fig. 5. Frequency-approach curves from dynamic nano-indentation.

Table 4 summarizes Young's modulus data from static and dynamic nano-indentation tests on various specimens. The static nano-indentation showed good results for bulk materials and micron-thick coatings, but a significant substrate effect for nano-coatings. The dynamic nano-indentation showed good results for all the specimens, including for ultra-thin films.

Nano-Scratch

The UNMT-1 Nano-analyzer module was used to measure hardness by nano-scratching, followed by AFM-like nano-imaging with the same tip. Its software allows for image analysis to obtain scratch depth profile along any direction of the nano-image. The hardness values were obtained from equation (1) above.

Table 4: Young's modulus data from static and dynamic nano-indentation		
Specimens	Young's Modulus, GPa	
	Nano-indenter	Nano-analyzer
Silicon 100	164±18	164±14
12 μm polymer on Si	6.85±0.07	6.0±0.5
2 μm polymer on Si	7.36±0.31	6.0±0.5
2 μm Ti on Si	98±13	98±10
2 μm DLC on Si	381±24	382±19
1 μm DLC on Si	372±29	379±21
100 nm DLC on Si	314±32*	370±25
4 nm DLC on Si	195±39*	361±27
Reference Polycarbonate	3.62±0.06	3.50±0.04
Reference Fused Silica	71.20±0.65	72.9±0.8
*Substrate effect		

Figure 6 shows an image of a 15 x 15 μm area of a 12 μm polymer coating, scratched under loads of 0.5, 0.2 and 0.1 mN (left to right). The scratch depth profiles along the X-X direction of Figure 6 are shown in Figure 7.

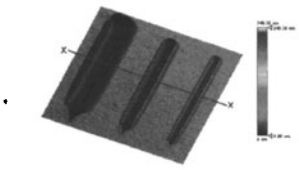

Fig.6. Nano-image of 3 nano-scratches

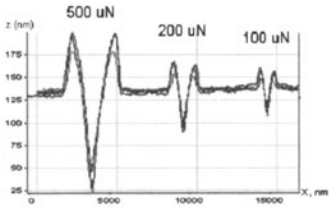

Fig.7. Three repeated scratch depth profiles

Table 5 summarizes data of nano-indentation *vs.* nano-scratch tests. The nano-indentation showed good results for micro-coatings, but a substrate effect (denoted as *) for nano-coatings. Such substrate effect was absent in the nano-scratch tests, when a stress distribution in the front of a moving indenter stays within the coating and does not extends into the substrate.

Table 5: Nanoindentation and Nano-scratch hardness data		
Specimens	Hardness, GPa	
	nano-indentation	nano-scratch
Silicon 100	11.4±1.8	11.6±1.0
12 μm polymer on Si	0.29±0.01	0.27±0.03
2 μm polymer on Si	0.44±0.01*	0.33+0.04
1 μm DLC on Si	30.5±2.9	31.2±1.7
100 nm DLC on Si	24.6±3.6*	30.8±1.7
4 nm DLC on Si	15.7±3.2*	29.1±1.9
Reference Polycarbonate	0.23±0.004	0.21±0.03
Reference Fused Silica	9.52±0.07	9.57±0.50

Scratch-Adhesion

Scratch-adhesion tests with a micro-indenter or a micro-blade are performed by sliding under a linearly increasing load (Fz). A failure of the coating is characterized by sudden change in coefficient of friction (COF) or contact high-frequency acoustic emission (AE). Figure 8 shows data from three scratch-adhesion tests with a diamond tip of 12.5 μm radius on a patterned LCD display with layers of indium-tin-oxide/overcoat/matrix on a glass substrate. At the load of about 16 mN, both COF and AE increased, indicating the failure. The periodic bumps in the COF and Fz plot were due to the rapid interactions of the tip with the patterned specimen. Table 6 shows the COF, AE and scratch-adhesion strength data of the top indium-tin-oxide layer.

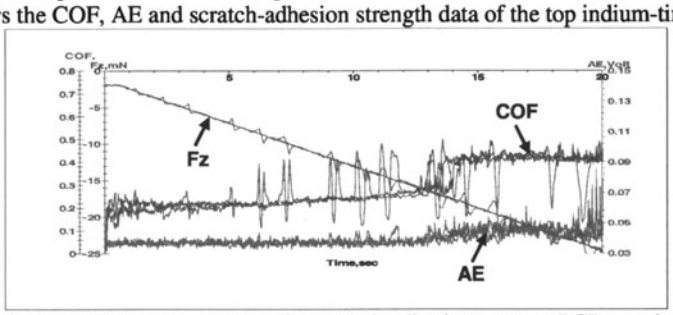

Fig.8. Fz, COF, and AE plots for scratch adhesion tests on LCD specimen.

Table 6: Scratch-adhesion data on LCD specimen

Adhesion Strength, mN	COF		AE	
	Before failure	After failure	Before failure	After failure
16.2	0.242	0.410	0.04	0.08
16.5	0.242	0.411	0.04	0.06
16.2	0.237	0.417	0.04	0.09
Mean : 16.3	**0.240**	**0.413**	**0.04**	**0.08**

CONCLUSIONS

The repeatable substrate-independent results were obtained in the indentation tests with the indents under 5-10% of film thickness and in the scratch tests with the scratches under 30-35% of film thickness. In the micro-indentation tests on metals, traditional Rockwell and Vickers hardness tests produced more data variability than the instrumented-hardness tests, though the statistics requires more data. The UNMT-1 provides a unique single platform for comparative studies of mechanical and tribological properties on micro- and nano-levels.

FUTURE STUDY

Next tests will be focused on indentation and scratch evaluation of coatings at extreme high and low temperatures, using UNMT-1 chamber modules.

REFERENCES

1. D. Tabor, Phil. Mag., **A74** (5), 1207 (1996).
2. N. Gitis, J. Xiao, and M. Vinogradov, J. ASTM Int. STP 1463, **2** (9), 80(2005).
3. N. Gitis, etc., Proc. Int. Joint Trib. Conf., San Diego, IJTC2007-44025 (2007)
4. W. Oliver and G. Pharr, J. Mat. Res., **19**(1), 1(2004); **7**, 1564(1992).

Mater. Res. Soc. Symp. Proc. Vol. 1049 © 2008 Materials Research Society 1049-AA02-07

Mechanical response of a single and released InP membrane

Eric Le Bourhis[1], and Gilles Patriarche[2]
[1]Laboratoire de Métallurgie Physique, Université de Poitiers, UMR 6630 CNRS, SP2MI-Téléport 2-Bd Marie et Pierre Curie, BP 30179, Futuroscope-chasseneuil Cedex, F-86962, France
[2]Laboratoire de Photonique et de Nanostructures, CNRS UPR 20, Marcoussis, 91460, France

ABSTRACT

InP membranes have been microfabricated and released on top of an InP substrate. The release process comprises membrane photolithography, interlayer sacrificial etching of a InP/InGaAs/InP substructure and drying with CO_2 at critical point. The mechanical response of the obtained small (40 µm) and thin (0.4 µm) membranes could be tested by nanoindentation. While keeping their epitaxial orientation through the fabrication process, delamination of the membrane was observed to occur before the indenting load reached 10 mN. Then cracking of the membrane was detected as a pop-in on the loading curves for loads larger than 10 mN.

INTRODUCTION

Mechanical behavior of single objects has attracted much interest in the past few years [1]. In this field, semiconductor defect and size engineering allows fabricating model structures. Moreover, indentation technique has proved to be powerful to test small volumes [2]. Originally, contact mechanics was developed for semi-infinite half space [3], this assumption being not fulfilled when the size of the plastic zone becomes of the order of one of the dimensions of the object [4-9]. 'Small' structures are expected to show a mechanical behavior deviating from that of a bulk. So far, length scale induced changes in the response of single semiconductor objects has been poorly addressed. Only recently were reported nanoindentation studies of GaAs single lines and of focused-ion beam (FIB) milled GaAs pillars in the µm-length scale [7-9]. Therefore, we decided to investigate the mechanical response of individual, small (40 µm in diameter) and thin (~ 0.4 µm) InP membranes. These were fabricated from InP/InGaAs/InP substructures and released on top of the InP substrate. Nanoindentation could be performed on these single membranes under increasing loads while interferential and transmission electron microscopies allowed getting deeper insight into the deformation of such small objects.

EXPERIMENT

Undoped (001) InP substrates were used for the study. InP membranes were micro fabricated and released on top of the InP substrate in a four step process. The first step was to grow an InP/InGaAs heterostructure on an InP substrate by low-pressure metal organic vapor phase epitaxy (MOVPE). The InGaAs layer was meant to be sacrificial and etched subsequently in order to release the membrane. Before this third step, the membranes were fabricated by photolithography of a poly-methyl methacrylate (PMMA)-based resin film previously deposited on top of the InP/InGaAs coated InP substrates. After the revealing step, a-SiN was deposited by plasma-enhanced chemical vapor deposition (PECVD). A lift-off process allowed producing a-SiN masks on the InP surface. Dry etching was then carried out with $SiCl_4$ plasma using a

reactive-ion-etching (RIE) machine. The a-SiN masks were then removed from the InP/InGaAs/InP substructures using a HF solution (end of the second step). The InGaAs sublayer was etched preferentially and the obtained structure later dried by CO_2 at critical point and released on the substrate (third and fourth steps). The thickness of the membranes was measured by profilometry using a DEKTAK 3 ST from VEECO. The membranes under study were determined to be about 400 nm thick while their diameter was about 40 µm. They were deformed by a Berkovich diamond pyramid using a NHT machine from CSEM (Switzerland) employing the X-Y tables to position the relevant area (membranes) under the tip. The tests were performed either on the membranes or on the bare substrates (Figure 1b) in the force-control mode of the machine. The calibration procedure suggested by Oliver and Pharr [10] was used to correct for the load-frame compliance of the apparatus and the imperfect shape of the indenter tip. A phase-shift interferometer (Micromap 570 ATOS, Pfungstadt, Germany) was used to obtain quantitative images of the surface topography. To prepare TEM plan-view thin foils of the indented samples, the undeformed side of the samples (back side) was mechanically and chemically thinned with a bromine-methanol solution until sufficiently thin to transmit the electron beam. The samples (indented surface) were observed in a Philips CM20-Super-Twin microscope operated at 200 kV equipped with a double-tilt sample holder (±28°).

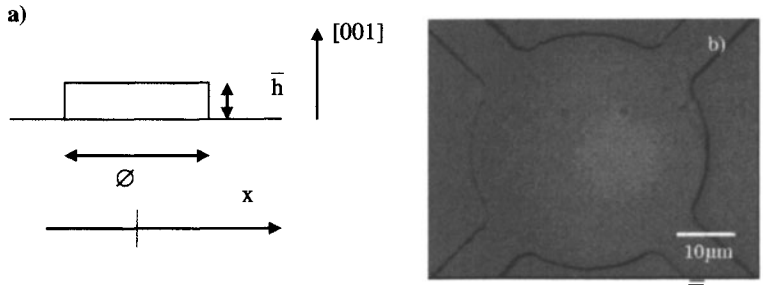

Figure 1: (a) Membrane geometric characteristics (diameter Ø, height $\bar{h}$). InP thin membrane surface is (001) while substrate is also (001) InP. (b) Membrane as indented under 10 mN. Note the crack appearing when the indent is made close to the membrane edge and only central indents were considered for the analysis.

RESULTS AND DISCUSSION

Figure 2 shows the loading and unloading curves obtained in the central part of a membrane under a maximum load F_{max} of 10 mN and at the reference surface (bare substrate). Slight differences on the indentation response are observed both on loading and unloading. The loading and most of the unloading curves are shifted to the right-hand side of the figure (larger penetrations) when the test is carried out on the central part of the membrane. The lowest portions of the unloading curves obtained on the reference surface and the membrane cross each other with a larger apparent recovery obtained in the case of a membrane. The maximum penetrations h_{max} and residual penetrations h_r of the indenter under a same maximum load of 10 mN are determined to be 315 ± 3 nm and 190 ± 10 nm on the membrane (± standard deviation of 10 events) and 305 ± 3 nm and 195 ± 3 nm on the bulk respectively. It is important to note that all these values remain below membrane thickness (400 nm) indicating that the interface